optica

Full rotational control of levitated silicon nanorods

Stefan Kuhn,[1,*,†] Alon Kosloff,[2,†] Benjamin A. Stickler,[3] Fernando Patolsky,[2] Klaus Hornberger,[3] Markus Arndt,[1] and James Millen[1]

[1]University of Vienna, Faculty of Physics, VCQ, Boltzmanngasse 5, 1090 Vienna, Austria
[2]School of Chemistry, Tel-Aviv University, Ramat-Aviv 69978, Israel
[3]University of Duisburg-Essen, Lotharstraße 1, 47048 Duisburg, Germany
*Corresponding author: stefan.kuhn@univie.ac.at

Optically levitated nano-objects in vacuum are among the highest quality mechanical oscillators, and thus of great interest for force sensing, cavity quantum optomechanics, and nanothermodynamic studies. These precision applications require exquisite control. Here, we present full control over the rotational and translational dynamics of an optically levitated silicon nanorod. We trap its center-of-mass and align it along the linear polarization of the laser field. The rod can be set into rotation at a predefined frequency by exploiting the radiation pressure exerted by elliptically polarized light. The rotational motion of the rod dynamically modifies the optical potential, which allows tuning of the rotational frequency over hundreds of kilohertz. Through nanofabrication, we can tailor all of the trapping frequencies and the optical torque, achieving reproducible dynamics that are stable over months, and analytically predict the motion with great accuracy. This first demonstration of full ro-translational control of nanoparticles in vacuum opens up the fields of rotational optomechanics, rotational ground state cooling, and the study of rotational thermodynamics in the underdamped regime.

1. INTRODUCTION

Nanofabrication has advanced all areas of science, technology, and medicine [1], including the field of optomechanics, where the motion of a mechanical oscillator is controlled by light. The quantum ground state of motion has been reached in optomechanical crystal devices [2] and superconducting microwave circuits [3]. Ground-state cooling enables the coherent transduction of signals [4], the production of non-classical states of light and matter [5], and the ultra-sensitive detection of motion [6] and forces [7]. Coherent optomechanical technology is limited by the coupling between the mechanical device and its environment, which leads to decoherence of quantum states, and by a reduction in mechanical quality factor due to clamping forces on the oscillator.

These limitations can be overcome by optically levitating the mechanical system such that it oscillates in a harmonic trapping potential. Optical trapping is applicable from atoms in vacuum [8,9] to complex organisms in liquid [10]. By optically levitating nanoscale objects in vacuum, ultra-high mechanical quality factors ($Q \sim 10^{12}$) are predicted [11], and it may be possible to generate macroscopic quantum superpositions [12]. Such massive quantum systems could test the limits of quantum physics [13,14], looking for the existence of new mechanisms of wave-function collapse such as spontaneous localization [15] or

gravitational effects [16–18]. Such goals require a high degree of control over all of the dynamics of the nanoparticle.

The field of levitated optomechanics is growing rapidly, with progress including feedback [19–21] and cavity cooling [22–25] to the millikelvin level and below, the sensing of forces on the zepto-Newton scale [26], and the study of Brownian motion [27] and equilibration [28] in the underdamped regime. Experiments are often limited by the quality of commercially available nanoparticles. Impurities lead to absorption of the trapping light, causing loss at low pressures [29], and even graphitization of levitated diamond [30]. Recently, rotation has been detected in levitated particles [31–34], displaying far greater rotation rates than experiments in liquid [35–38].

In this work, we trap clean, nanofabricated silicon nanorods and study their center-of-mass and rotational motion. Our particles are of uniform, tailored size and shape, allowing a high degree of repeatability, predictability, and control of the dynamics. We are able to trap the nanorods, trap and control their orientation, and tunably spin them using the radiation pressure exerted by the light field. While rotational control has been achieved in liquid [35–37,39,40], this is the first demonstration of trapping nanorods in vacuum, to the best of our knowledge, and we observe novel features such as shape enhanced light–matter

interactions and dynamic reshaping of the trapping potential. Such full control opens the way to optomechanical rotational cooling [34,41,42], even to the quantum level [42].

2. EXPERIMENTAL SETUP

A single silicon nanorod is optically trapped in the focus formed by two counterpropagating laser beams of wavelength $\lambda = 1550$ nm; see Fig. 1(a). At this wavelength, silicon exhibits a high relative permittivity, $\epsilon_r = 12$, and negligible absorption, which is supported by the fact that we see no signature of heating due to light absorption (following the method in Ref. [29]). The nanorods are tailored to have a length of $\ell = (725 \pm 15)$ nm and a diameter of $d = (130 \pm 13)$ nm, corresponding to a mass $M = (1.3 \pm 0.3) \times 10^{10}$ amu. They are fabricated onto a silicon chip following the methods described in Ref. [33]. The laser trap is characterized by a beam waist radius $w_0 \approx 27$ μm and the total power $P_{\text{tot}} = 1.35$ W, making a large volume trap to enhance the rate of capture. The nanorods are trapped in a clean N_2 environment at a pressure of $p_g = 4$ mbar, after being launched by laser desorption from a silicon wafer; see Refs. [33,43]. Up to 10 nanorods are simultaneously trapped, and we perturb the trapping field until a single nanorod remains. The rods can be stably trapped for months at any pressure above 1 mbar, below which they are lost, as observed in experiments with spherical nanoparticles [22,29].

3. TRAPPING THE NANORODS

The motional state of the nanorod is described by its center-of-mass position (x, y, z) and by its orientation (α, β) [see Fig. 1(b)], where x points counter-parallel to the direction of gravity and
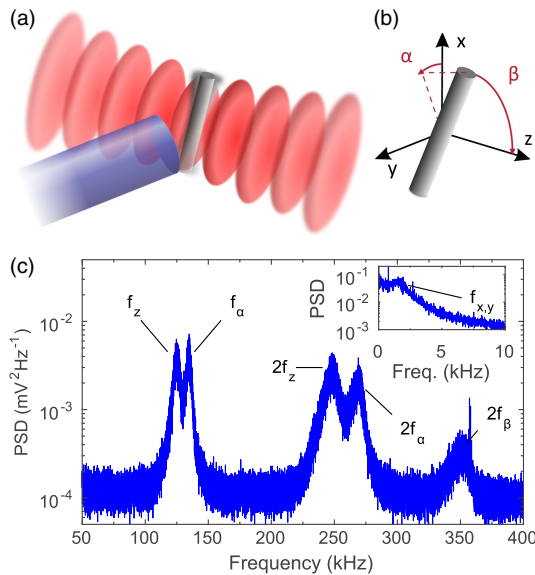

Fig. 1. (a) Nanofabricated silicon nanorods of length $\ell \simeq (725 \pm 15)$ nm and diameter $d \simeq (130 \pm 13)$ nm are optically levitated in a standing laser wave at low pressures. The light they scatter is collected by a multimode optical fiber placed close to the trap waist. (b) The rods have five degrees of freedom that can be controlled: three translational (x, y, z) and two rotational (α, β). (c) By monitoring the scattered light, trapping of all five degrees of freedom can be observed in the PSD when the trap light is linearly polarized. These data were acquired at a pressure of 4 mbar. The appearance of the various harmonics can be explained by slight misalignment of the trap as discussed in Supplement 1.

z along the beam axis. The orientation of the rod is parametrized by α, the angle between the x axis and the projection of the rod onto the x–y plane, and β the angle between the rod's symmetry axis and the beam propagation axis. The motion of the nanorod is measured via the light that the rod scatters out of the trap, which is collected with a 1 mm diameter multimode optical fiber as described in Ref. [33].

The polarization of the two trapping beams determines the properties of the optical trap. In the case of co-linear polarization, the rod aligns with the field polarization and is thus trapped in all its degrees of freedom. The resulting trapping frequencies can be measured in the power spectral density (PSD) of the scattered light signal, as shown in Fig. 1(c). Using a LiNb-polarization controller, we can perform arbitrary wave-plate operations on the polarization of the trapping light [44]. The optical setup [see Fig. 2(a)] is designed such that the rod experiences the same polarization from both arms of the counterpropagating trap. By realizing a half-wave-plate operation on the linearly polarized trapping beam we can align the rod along any direction orthogonal to the trap axis, as has been observed in liquid [36].

The trapping frequencies of a harmonically captured rod can be calculated as [42]

$$f_{x,y} = \frac{1}{2\pi}\sqrt{\frac{8P_{\text{tot}}\chi_\parallel}{\pi\varrho c w_0^4}}, \qquad f_z = \frac{1}{2\pi}\sqrt{\frac{4P_{\text{tot}}\chi_\parallel k^2}{\pi\varrho c w_0^2}},$$

$$f_\beta = \frac{1}{2\pi}\sqrt{\frac{48P_{\text{tot}}\chi_\parallel}{\pi\varrho c w_0^2\ell^2}\left(\frac{\Delta\chi}{\chi_\parallel} + \frac{(k\ell)^2}{12}\right)},$$

$$f_\alpha = \frac{1}{2\pi}\sqrt{\frac{48P_{\text{tot}}\Delta\chi}{\pi\varrho c w_0^2\ell^2}}, \tag{1}$$

where $k = 2\pi/\lambda$, $\varrho = 2330$ kg m^{-3} is the density of silicon, $\chi_\parallel = \epsilon_r - 1$ is the susceptibility along the rod's symmetry axis, and $\Delta\chi = (\epsilon_r - 1)^2/(\epsilon_r + 1)$ is the susceptibility anisotropy [45]. At the maximum input power we measure $f_{x,y} = (1.6 \pm 0.2)$ kHz, $f_z = (124 \pm 1)$ kHz, $f_\alpha = (134 \pm 1)$ kHz, and $f_\beta = (175.0 \pm 0.5)$ kHz; see Fig. 1(c). For comparison, a silicon nanosphere of the same volume under the same experimental conditions would have $f_z = 58$ kHz, and a silica sphere would have $f_z = 47$ kHz, illustrating the great potential for silicon nanorods in cavity cooling experiments [42]. We can use the measured frequencies to deduce the trapping waist radius $w_0 = (27 \pm 3)$ μm, which is the only free experimental parameter. The measured frequencies agree well with the theoretical expectations, as shown in Fig. 3(c). The slight (<5%) discrepancy between the measured and predicted value of f_β is attributed to the fact that the rods have finite diameter and the generalized Rayleigh–Gans approximation [42] is not strictly valid.

4. SPINNING THE NANORODS

When the trapping light is circularly polarized, the trapping potential for the α motion vanishes while the standing wave structure along z is retained. The radiation pressure of the laser field exerts a constant torque N_α acting on α. Adapting the theory presented in Ref. [42], the resulting torque is obtained as

$$N_\alpha = \frac{P_{\text{tot}}\Delta\chi\ell^2 d^4 k^3}{48c w_0^2}[\Delta\chi\eta_1(k\ell) + \chi_\perp\eta_2(k\ell)], \tag{2}$$

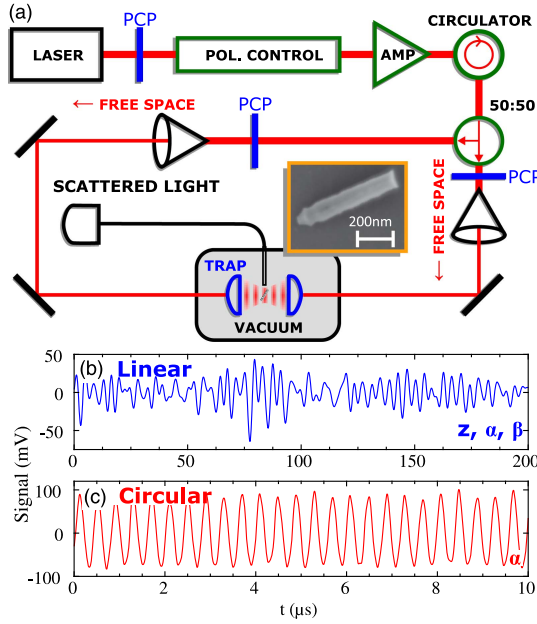where the two functions $\eta_{1,2}(k\ell)$ are given by

Fig. 2. (a) Experimental setup. Light at $\lambda = 1550$ nm is produced by a fiber laser (Keysight 81663A), and then goes through an electro-optical in-fiber polarization controller (EOSPACE), allowing us to realize arbitrary wave-plate operations. The light is amplified in a fiber amplifier (Hangzhou Huatai Optic HA5435B-1) and split equally to make the two arms of the trap. Stress-induced birefringence in the fibers can be accounted for with polarization controlling paddles (PCPs). The system is completely fiber-based until out-coupled to the aspheric trapping lenses ($f = 20$ mm). The inset shows a scanning electron microscopy micrograph of a rod that was launched and captured on a sample plate. The scattered light signal reveals the nanorod dynamics in case of (b) co-linear polarization, and (c) the strongly driven rotation of the rod for circularly polarized trapping light.

$$\eta_1(k\ell) = \frac{3}{4}\int_{-1}^{1} d\xi(1-\xi^2)\mathrm{sinc}^2\left(\frac{k\ell\xi}{2}\right),$$

$$\eta_2(k\ell) = \frac{3}{8}\int_{-1}^{1} d\xi(1-3\xi^2)\mathrm{sinc}^2\left(\frac{k\ell\xi}{2}\right). \qquad (3)$$

For short rods, $k\ell \ll 1$, one has $\eta_1 \simeq 1$, while $\eta_2 \simeq 0$.

Collisions with residual gas molecules lead to damping of the rotational motion. Since the mean free path of the gas molecules exceeds the diameter of the rod (free molecular regime [46]), the rotational damping rate for diffuse reflection of gas molecules of mass m_g takes the form [47]

$$\Gamma = \frac{d\ell p_g}{2M}\sqrt{\frac{2\pi m_g}{k_B T}}\left(\frac{3}{2}+\frac{\pi}{4}\right), \qquad (4)$$

where T is the gas temperature.

The maximum steady-state rotation frequency is obtained by balancing the torque Eq. (2) with the damping Eq. (4),

$$f_{\alpha,\max} = \frac{N_\alpha}{2\pi I\Gamma}, \qquad (5)$$

with $I = M\ell^2/12$ the rod's moment of inertia. This expression agrees well with the measured value of the rotation frequency $f_{\alpha,\mathrm{rot}}$ as a function of power and pressure, as shown in Figs. 3(d) and 3(e), respectively.

A comparison of the PSD for the co-linear and the circular polarization traps is shown in Fig. 3(c). The peak related to the trapping frequency at f_α vanishes and a pronounced peak at $2f_{\alpha,\mathrm{rot}}$ arises. We are sensitive only to $2f_{\alpha,\mathrm{rot}}$ due to the symmetry of the rod. The rotation of the rod in the circularly polarized field results in a reduced average susceptibility and thus a weaker trapping potential, which shifts the axial trapping frequency to $f_{z,\mathrm{rot}} = 94$ kHz as discussed in Supplement 1. The rapid rotation in α leads to a stabilization in β and hence the
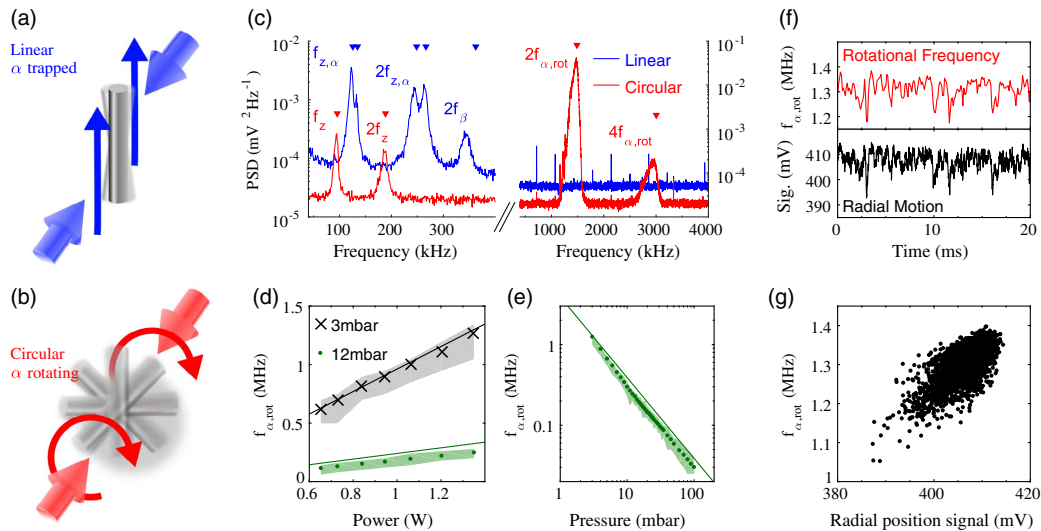

Fig. 3. Comparing the dynamics when the nanorod is (a) trapped in all degrees of freedom by linearly polarized light and (b) driven to rotate in the α direction by circularly polarized light. (c) The PSD for circularly (red) and linearly (blue) polarized light. For circular polarization, the trapping frequency f_α vanishes, and the rotational frequency $f_{\alpha,\mathrm{rot}}$ appears. The peak at f_β vanishes since the motion in β is stabilized when the rod is spinning. Markers indicate predicted trapping frequencies. The rotational frequency scales (d) linearly with power, and (e) decreases with increasing pressure, as predicted by Eq. (5). Markers represent the mean value of $f_{\alpha,\mathrm{rot}}$, the shaded areas represent the full range of $f_{\alpha,\mathrm{rot}}$, and solid lines are the theoretically expected maximal value of $f_{\alpha,\mathrm{rot}}$. The broad frequency distribution of $f_{\alpha,\mathrm{rot}}$ is due to coupling between the motion in α and x, y (radial). (f) Perturbations from the equilibrium position (lower panel) are reflected in instantaneous frequency fluctuations (top panel). (g) The correlation between the radial position and $f_{\alpha,\mathrm{rot}}$.

complete suppression of the peak at f_β in Fig. 3(c). A similar effect has also been observed for spinning microspheres [32].

The broad distribution of frequencies about $2f_{\alpha,\text{rot}}$ is due to perturbations temporarily decreasing the rotation rate, which then takes time to spin back up to the maximum value. For example, irregular excursions in the radial x, y directions lead to variations in the instantaneous rotation frequency via variation in the local light intensity, as shown in Fig. 3(f), with the correlation clearly shown in Fig. 3(g). The maximum rotation rate is limited by pressure in this setup, with an ultimate limit presumably set by material properties. In previous work, rotation rates of 50 MHz were observed for free nanorods in ultra high vacuum (UHV) [33].

5. TUNING THE ROTATIONAL FREQUENCY

To study the effect of driven rotation in more detail we use the polarization controller to perform a quarter-wave-plate (QWP) operation on the trapping light and track the motion of the rod at each setting; see Fig. 4. Starting from a linear polarization along x and increasing its ellipticity at first leads to a shift of all trapping frequencies to lower values due to a reduced trap depth, as shown in Fig. 4(a). At a QWP setting of 30°, the radiation pressure induced torque starts driving the rod into rotation over the trapping potential in the direction of α, the frequencies $f_{\alpha,\beta}$ vanish, and f_z drops to a steady value of $f_{z,\text{rot}} = (94 \pm 1)$ kHz, as also seen in Fig. 3(c). Rotating beyond 45°, one may expect the nanorod to become trapped again at 60°; however, the rod is not trapped until 85°. When starting at 90° and decreasing the QWP angle, the rod spins at 60° and is not trapped until 5°, showing a symmetric hysteresis; see Fig 4(b).

This effect is due to the anisotropy of the susceptibility tensor: a trapped rod experiences the full trap depth related to $\chi_\parallel$, whereas the trapping potential for a spinning rod is proportional to the susceptibility averaged over rotations in the 2D plane orthogonal to the beam axis $(\chi_\parallel + \chi_\perp)/2$, which is smaller by a factor of 1.7. Thus, it requires a greater torque to spin a trapped rod than to maintain the rotation of an already spinning rod. The value of $f_{\alpha,\text{rot}}$ varies with the ellipticity of the light, as shown in Fig. 4(b).
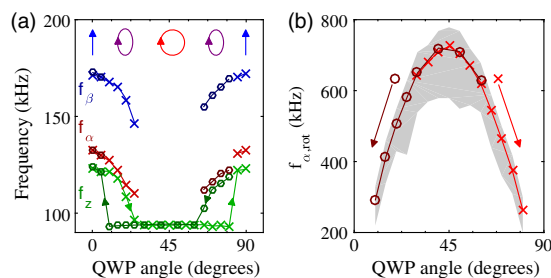

Fig. 4. Effect of performing a QWP operation on the trapping light at 5 mbar, either increasing from 0° (crosses) or decreasing from 90° (circles). At 0° and 90° the trap is linearly polarized along the y axis. At 45° the polarization is circular. (a) Shift of the trapping frequencies for different QWP settings. For small deviations from linear polarization the trapping frequencies decrease due to a lower trapping potential. At 30° from the starting linear polarization, the light is circularly polarized enough to drive $f_{\alpha,\text{rot}}$, at which point $f_{\alpha,\beta}$ vanish, and f_z drops. At 85° from the starting linear polarization, the motion becomes trapped again. (b) Because of this hysteresis the driven rotational frequency $f_{\alpha,\text{rot}}$ can be tuned over several hundred kilohertz via the ellipticity of the trapping field. The markers indicate the mean value of $f_{\alpha,\text{rot}}$, and the shaded region represents the range of measured frequencies.

By exploiting the dynamical modification of the trap depth we can extend the range over which the rotation frequency can be tuned to many hundreds of kilohertz.

6. CONCLUSIONS

In summary, we present a method to capture and levitate nanofabricated silicon nanorods at low pressures, working with telecom wavelengths in a fiber-based setup. We can precisely control the length and diameter of our nanorods, meaning we can tailor rods to attain particular trapping and rotational frequencies. We are able to trap all relevant degrees of freedom, and control the orientation of the rods via the polarization of the trapping beams. By using circularly polarized light we can spin the nanorods at more than 1 MHz, and tune this frequency over hundreds of kilohertz by introducing ellipticity into the field polarization and through a dynamic modification of the trapping potential. When the rod is spinning we notice a stabilization of the tilt angle β and a coupling to the radial motion x, y. The system is very well understood as documented in the excellent agreement between experiment and theory. The high degree of control opens the way to study rotational optomechanics [48–50], orientational decoherence [51,52], rotational underdamped Brownian motion, and stochastic thermodynamics, and synchronization of multiple rotors due to optical binding [53]. This is the first use of silicon in an optical trap in vacuum, and its high susceptibility and low absorption in this frequency band, combined with the shape-enhanced susceptibility of rods, will enable rotational cavity cooling to the quantum level [34,42]. Such deeply trapped, cooled particles may be used as point sources for orientation-dependent interference experiments [54,55].

†Co-first authors.

See Supplement 1 for supporting content.

REFERENCES

1. B. Bhushan, *Springer Handbook of Nanotechnology* (Springer, 2010).
2. J. Chan, T. P. Mayer Alegre, A. H. Safavi-Naeini, J. T. Hill, A. Krause, S. Gröblacher, M. Aspelmeyer, and O. Painter, "Laser cooling of a nanomechanical oscillator into its quantum ground state," Nature **478**, 89–92 (2011).
3. J. D. Teufel, T. Donner, D. Li, J. W. Harlow, M. S. Allman, K. Cicak, A. J. Sirois, J. D. Whittaker, K. W. Lehnert, and R. W. Simmonds, "Sideband cooling of micromechanical motion to the quantum ground state," Nature **475**, 359–363 (2011).
4. J. Bochmann, A. Vainsencher, D. D. Awschalom, and A. N. Cleland, "Nanomechanical coupling between microwave and optical photons," Nat. Phys. **9**, 712–716 (2013).
5. R. Riedinger, S. Hong, R. A. Norte, J. A. Slater, J. Shang, A. G. Krause, V. Anant, M. Aspelmeyer, and S. Gröblacher, "Non-classical correlations between single photons and phonons from a mechanical oscillator," Nature **530**, 313–316 (2016).

6. O. Arcizet, P. F. Cohadon, T. Briant, M. Pinard, A. Heidmann, J. M. MacKowski, C. Michel, L. Pinard, O. Français, and L. Rousseau, "High-sensitivity optical monitoring of a micromechanical resonator with a quantum-limited optomechanical sensor," Phys. Rev. Lett. **97**, 133601 (2006).

7. A. G. Krause, M. Winger, T. D. Blasius, Q. Lin, and O. Painter, "A high-resolution microchip optomechanical accelerometer," Nat. Photonics **6**, 768–772 (2012).

8. W. D. Phillips, "Nobel Lecture: laser cooling and trapping of neutral atoms," Rev. Mod. Phys. **70**, 721–741 (1998).

9. N. Schlosser, G. Reymond, I. Protsenko, and P. Grangier, "Sub-Poissonian loading of single atoms in a microscopic dipole trap," Nature **411**, 1024–1027 (2001).

10. A. Ashkin and J. M. Dziedzic, "Optical trapping and manipulation of viruses and bacteria," Science **235**, 1517–1520 (1987).

11. D. E. Chang, C. A. Regal, S. B. Papp, D. J. Wilson, J. Ye, O. Painter, H. J. Kimble, and P. Zoller, "Cavity opto-mechanics using an optically levitated nanosphere," Proc. Natl. Acad. Sci. USA **107**, 1005–1010 (2010).

12. O. Romero-Isart, M. Juan, R. Quidant, and J. Cirac, "Toward quantum superposition of living organisms," New J. Phys. **12**, 033015 (2010).

13. M. Arndt and K. Hornberger, "Insight review: testing the limits of quantum mechanical superpositions," Nat. Phys. **10**, 271–277 (2014).

14. J. Bateman, S. Nimmrichter, K. Hornberger, and H. Ulbricht, "Near-field interferometry of a free-falling nanoparticle from a point-like source," Nat. Commun. **5**, 4788 (2014).

15. G. C. Ghirardi, P. Pearle, and A. Rimini, "Markov processes in Hilbert space and continuous spontaneous localization of systems of identical particles," Phys. Rev. A **42**, 78–89 (1990).

16. L. Diósi, "A universal master equation for the gravitational violation of quantum mechanics," Phys. Lett. A **120**, 377–381 (1987).

17. G. C. Ghirardi, R. Grassi, and A. Rimini, "Continuous-spontaneous-reduction model involving gravity," Phys. Rev. A **42**, 1057–1064 (1990).

18. R. Penrose, "On gravity's role in quantum state reduction," Gen. Relativity Gravitation **28**, 581–600 (1996).

19. T. Li, S. Kheifets, and M. G. Raizen, "Millikelvin cooling of an optically trapped microsphere in vacuum," Nat. Phys. **7**, 527–530 (2011).

20. J. Gieseler, B. Deutsch, R. Quidant, and L. Novotny, "Subkelvin parametric feedback cooling of a laser-trapped nanoparticle," Phys. Rev. Lett. **109**, 103603 (2012).

21. J. Vovrosh, M. Rashid, D. Hempston, J. Bateman, and H. Ulbricht, "Controlling the motion of a nanoparticle trapped in vacuum," arXiv:1603.02917 (2016).

22. N. Kiesel, F. Blaser, U. Delic, D. Grass, R. Kaltenbaek, and M. Aspelmeyer, "Cavity cooling of an optically levitated nanoparticle," Proc. Natl. Acad. Sci. USA **110**, 14180–14185 (2013).

23. P. Asenbaum, S. Kuhn, S. Nimmrichter, U. Sezer, and M. Arndt, "Cavity cooling of free silicon nanoparticles in high-vacuum," Nat. Commun. **4**, 2743 (2013).

24. J. Millen, P. Z. G. Fonseca, T. Mavrogordatos, T. S. Monteiro, and P. F. Barker, "Cavity cooling a single charged levitated nanosphere," Phys. Rev. Lett. **114**, 123602 (2015).

25. P. Z. G. Fonseca, E. B. Aranas, J. Millen, T. S. Monteiro, and P. F. Barker, "Nonlinear dynamics and millikelvin cavity-cooling of levitated nanoparticles," Phys. Rev. Lett. **117**, 173602 (2016).

26. G. Ranjit, M. Cunningham, K. Casey, and A. A. Geraci, "Zeptonewton force sensing with nanospheres in an optical lattice," Phys. Rev. A **93**, 053801 (2016).

27. T. Li, S. Kheifets, D. Medellin, and M. G. Raizen, "Measurement of the instantaneous velocity of a Brownian particle," Science **328**, 1673–1675 (2010).

28. J. Gieseler, R. Quidant, C. Dellago, and L. Novotny, "Dynamic relaxation of a levitated nanoparticle from a non-equilibrium steady state," Nat. Nanotech. **9**, 358–364 (2014).

29. J. Millen, T. Deesuwan, P. Barker, and J. Anders, "Nanoscale temperature measurements using non-equilibrium Brownian dynamics of a levitated nanosphere," Nat. Nanotech. **9**, 425–429 (2014).

30. A. T. M. A. Rahman, A. C. Frangeskou, M. S. Kim, S. Bose, G. W. Morley, and P. F. Barker, "Burning and graphitization of optically levitated nanodiamonds in vacuum," Sci. Rep. **6**, 21633 (2016).

31. B. Kane, "Levitated spinning graphene flakes in an electric quadrupole ion trap," Phys. Rev. B **82**, 115441 (2010).

32. Y. Arita, M. Mazilu, and K. Dholakia, "Laser-induced rotation and cooling of a trapped microgyroscope in vacuum," Nat. Commun. **4**, 2374 (2013).

33. S. Kuhn, P. Asenbaum, A. Kosloff, M. Sclafani, B. A. Stickler, S. Nimmrichter, K. Hornberger, O. Cheshnovsky, F. Patolsky, and M. Arndt, "Cavity-assisted manipulation of freely rotating silicon nanorods in high vacuum," Nano Lett. **15**, 5604–5608 (2015).

34. T. M. Hoang, Y. Ma, J. Ahn, J. Bang, F. Robicheaux, Z.-Q. Yin, and T. Li, "Torsional optomechanics of a levitated nonspherical nanoparticle," Phys. Rev. Lett. **117**, 123604 (2016).

35. M. E. J. Friese, T. A. Nieminen, N. R. Heckenberg, and H. Rubinsztein-Dunlop, "Optical alignment and spinning of laser-trapped microscopic particles," Nature **394**, 348–350 (1998).

36. L. Tong, V. D. Miljkovic, and M. Kall, "Alignment, rotation, and spinning of single plasmonic nanoparticles and nanowires using polarization dependent optical forces," Nano Lett. **10**, 268–273 (2010).

37. A. Lehmuskero, R. Ogier, T. Gschneidtner, P. Johansson, and M. Käll, "Ultrafast spinning of gold nanoparticles in water using circularly polarized light," Nano Lett. **13**, 3129–3134 (2013).

38. L. Shao, Z.-J. Yang, D. Andrén, P. Johansson, and M. Käll, "Gold nanorod rotary motors driven by resonant light scattering," ACS Nano **9**, 12542–12551 (2015).

39. F. Borghese, P. Denti, R. Saija, M. Iatì, and O. Maragò, "Radiation torque and force on optically trapped linear nanostructures," Phys. Rev. Lett. **100**, 163903 (2008).

40. P. H. Jones, F. Palmisano, F. Bonaccorso, P. G. Gucciardi, A. Calogero, A. C. Ferrari, and O. M. Marago, "Rotation detection in light-driven nanorotors," ACS Nano **3**, 3077–3084 (2009).

41. M. Bhattacharya and P. Meystre, "Using a Laguerre-Gaussian beam to trap and cool the rotational motion of a mirror," Phys. Rev. Lett. **99**, 153603 (2007).

42. B. A. Stickler, S. Nimmrichter, L. Martinetz, S. Kuhn, M. Arndt, and K. Hornberger, "Rotranslational cavity cooling of dielectric rods and disks," Phys. Rev. A **94**, 033818 (2016).

43. J. Millen, S. Kuhn, F. Patolsky, A. Kosloff, and M. Arndt, "Cooling and manipulation of nanoparticles in high vacuum," Proc. SPIE **9922**, 99220C (2016).

44. A. J. P. Van Haasteren, H. J. Frankena, J. J. G. M. Vandertol, and M. O. van Deventer, "Modeling and characterization of an electrooptic polarization controller on LiNbO₃," J. Lightwave Technol. **11**, 1151–1157 (1993).

45. H. van de Hulst, *Light Scattering by Small Particles* (Dover, 1981).

46. C. Cercignani, *Theory and Application of the Boltzmann Equation* (Scottish Academic, 1975).

47. A. D. Eisner and I. Gallily, "On the stochastic nature of the motion of non-spherical aerosol particles: III. The rotational diffusion diadic and applications," J. Colloid Interface Sci. **81**, 214–233 (1981).

48. J. T. Rubin and L. I. Deych, "Optical forces due to spherical microresonators and their manifestation in optically induced orbital motion of nanoparticles," Phys. Rev. A **84**, 023844 (2011).

49. M. Bhattacharya, "Rotational cavity optomechanics," J. Opt. Soc. Am. B **32**, B55 (2015).

50. H. Shi and M. Bhattacharya, "Optomechanics based on angular momentum exchange between light and matter," J. Phys. B **49**, 153001 (2015).

51. B. A. Stickler, B. Papendell, and K. Hornberger, "Spatio-orientational decoherence of nanoparticles," Phys. Rev. A **94**, 033828 (2016).

52. C. Zhong and F. Robicheaux, "Decoherence of rotational degrees of freedom," Phys. Rev. A **94**, 052109 (2016).

53. S. H. Simpson, L. Chvátal, and P. Zemánek, "Synchronization of colloidal rotors through angular optical binding," Phys. Rev. A **93**, 023842 (2016).

54. B. W. Shore, P. Dömötör, E. Sadurní, G. Süssmann, and W. P. Schleich, "Scattering of a particle with internal structure from a single slit," New J. Phys. **17**, 013046 (2015).

55. B. A. Stickler and K. Hornberger, "Molecular rotations in matter-wave interferometry," Phys. Rev. A **92**, 023619 (2015).